ACS OMEGA

Article

http://pubs.acs.org/journal/acsodf

Polypropylene/Layered Double Hydroxide Nanocomposites: Influence of LDH Intralayer Metal Constituents on the Properties of Polypropylene

Baku Nagendra,[†,‡] C. V. Sijla Rosely,[†,‡] Andreas Leuteritz,[§] Uta Reuter,[§] and E. Bhoje Gowd*[,†,‡]

[†]Materials Science and Technology Division, CSIR-National Institute for Interdisciplinary Science and Technology, Trivandrum 695019, Kerala, India

[‡]Academy of Scientific and Innovative Research (AcSIR), New Delhi 110001, India

[§]Leibniz-Institut für Polymerforschung Dresden e.V., Hohe Strasse 6, D-01069 Dresden, Germany

Supporting Information

ABSTRACT: Sonication-assisted delamination of layered double hydroxides (LDHs) resulted in smaller-sized LDH nanoparticles (~50−200 nm). Such delaminated Co−Al LDH, Zn−Al LDH, and Co−Zn−Al LDH solutions were used for the preparation of highly dispersed isotactic polypropylene (iPP) nanocomposites. Transmission electron microscopy and wide-angle X-ray diffraction results revealed that the LDH nanoparticles were well dispersed within the iPP matrix. The intention of this study is to understand the influence of the intralayer metal composition of LDH on the various properties of iPP/LDH nanocomposites. The sonicated LDH nanoparticles showed a significant increase in the crystallization rate of iPP; however, not much difference in the crystallization rate of iPP was observed in the presence of different types of LDH. The dynamic mechanical analysis results indicated that the storage modulus of iPP was increased significantly with the addition of LDH. The incorporation of different types of LDH showed no influence on the storage modulus of iPP. But considerable differences were observed in the flame retardancy and thermal stability of iPP with the type of LDH used for the preparation of nanocomposites. The thermal stability (50% weight loss temperature ($T_{0.5}$)) of the iPP nanocomposite containing three-metal LDH (Co−Zn−Al LDH) is superior to that of the nanocomposites made of two-metal LDH (Co−Al LDH and Zn−Al LDH). Preliminary studies on the flame-retardant properties of iPP/LDH nanocomposites using microscale combustion calorimetry showed that the peak heat release rate was reduced by 39% in the iPP/Co−Zn−Al LDH nanocomposite containing 6 wt % LDH, which is higher than that of the two-metal LDH containing nanocomposites, iPP/Co−Al LDH (24%) and iPP/Zn−Al LDH (31%). These results demonstrated that the nanocomposites prepared using three-metal LDH showed better thermal and flame-retardant properties compared to the nanocomposites prepared using two-metal LDH. This difference might be due to the better char formation capability of three-metal LDH compared to that of two-metal LDH.

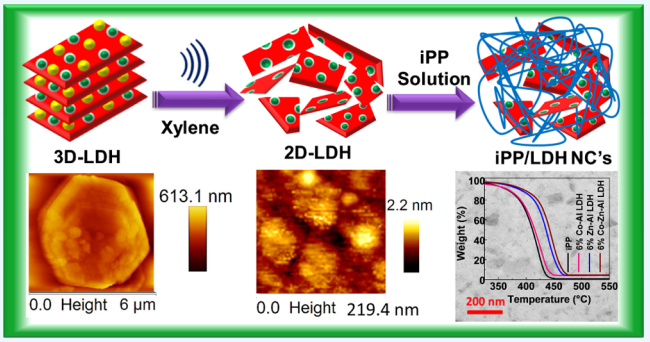

INTRODUCTION

Layered materials are an interesting class of compounds, consisting of a two-dimensional (2D) sheet-like structure with strong bindings within the individual layer and weak van der Waals forces between the layers.[1−4] The weak interaction between these layers allows them to be exfoliated or delaminated into ultrathin 2D nanosheets. These ultrathin nanomaterials have gained significant interest after the discovery of exfoliated graphene from graphite.[5] Dozens of 2D nanomaterials have been reported in the last few years, including transition metal oxides, transition metal dichalcogenides, hexagonal boron nitride, synthetic silicate clays, layered metal oxides, layered double hydroxides (LDHs), etc.[3,6−9] Because of the promising applications of these ultrathin 2D nanomaterials, a large number of synthetic methods, such as mechanical cleavage,[5,10] chemical vapor deposition,[11] ion-intercalation and exfoliation,[2] liquid exfoliation,[3,6] etc., have been developed.

Polymer matrices filled with nanosized particles have drawn widespread attention of researchers due to the promise of combining the superior thermal and mechanical properties of nanoparticles with the flexibility and processability of polymers.[7−9,12−16] The performance of the nanocomposites depends on many factors, such as the degree of dispersion of nanoparticles in the polymer matrix, compatibility between the nanoparticles and polymer, and the aspect ratio of the

Received: December 13, 2016
Accepted: December 21, 2016
Published: January 4, 2017

DOI: 10.1021/acsomega.6b00485
ACS Omega 2017, 2, 20−31

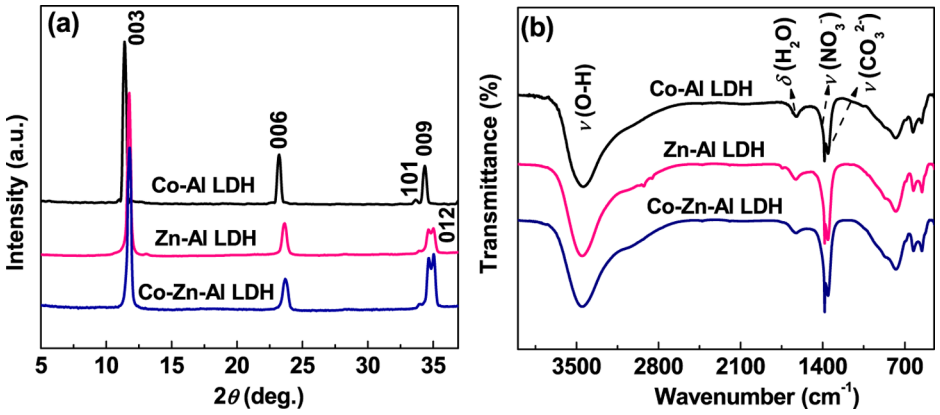

Figure 1. (a) Powder XRD patterns and (b) FTIR spectra of as-prepared Co−Al LDH, Zn−Al LDH, and Co−Zn−Al LDH.

nanofillers used.[7−9,12−14] In recent years, a range of layered materials of varying dimensions have been used as nanofillers in the preparation of polymer nanocomposites due to their exciting properties.[7−9,12,14,15]

In recent times, LDHs, also known as anionic clays, are considered to be an emerging class of layered nanofillers for the preparation of polymer nanocomposites.[7,15−32] The flexibility in tuning the type of metal ions in inorganic layers, as well as balancing anions in the interlayer space (easily exchangeable with other anionic species), enables these materials to find many applications, including in catalysis, pharmaceuticals, UV absorbents, CO_2 adsorbents, and flame-retardant additives.[7,17,18,33,34] The exfoliation of LDH in the polymer matrix is always a challenge because of the stronger interlayer electrostatic interactions. Recently, liquid exfoliation of LDH has drawn increasing attention as a process to produce ultrathin nanosheets with drastically improved surface activity.[4,18,21,28,35,36] This method is preferred over the other methods by polymer scientists, as the aggregation of exfoliated nanosheets can be prevented by polymers, which results in the formation of highly dispersed polymer/LDH nanocomposites by the solution blending method.[18,21,36,37] Moreover, this method does not require the prior modification of LDH with organic modifiers or surfactants. The degree of dispersion and the exfoliation of layered materials in polymer matrices have been shown to improve optical, thermal, rheological, flame retardancy, and mechanical properties of the base polymer.[7,18,22,23,31,37]

Recently, highly dispersed polymer/LDH nanocomposites have been prepared by the liquid exfoliation method. Wang et al. converted the hydrophilic LDH layers to hydrophobic ones by an aqueous miscible organic solvent treatment (AMOST) and prepared the stable dispersions of LDH in nonpolar solvents.[21,28,36,38] Subsequently, the exfoliated LDH nanosheets were used to prepare polypropylene/LDH nanocomposites by the solution blending method.[21,28] Using this method, it was shown that the PP nanocomposites prepared with Zn_2Al-borate displayed better performance than the nanocomposites prepared with the equivalent Mg_3Al-borate.[28] In another study, Wang and co-workers revealed that the gallery anions resulted in a significant difference in the properties of the polymer/LDH nanocomposites.[37] The synergistic effect of different LDH with the combination of an intumescent flame-retardant additive was studied by the melt blending method, and it was shown that the nanocomposite containing ternary LDH is a better flame-retardant additive.[39] Recently, we have reported highly dispersed isotactic polypropylene (iPP)/LDH nanocomposites using two different-sized (lateral size) LDH and showed that the lateral size of the LDH has a significant influence on the thermal stability and crystallization rate of iPP.[18]

Here, we prepared iPP/LDH nanocomposites filled with three different types of LDH (Co−Al LDH, Zn−Al LDH, and Co−Zn−Al LDH) by the solvent mixing method, particularly using the sonicated LDH (fragmented LDH). Both LDH and iPP/LDH nanocomposites were carefully characterized by transmission electron microscopy (TEM), atomic force microscopy (AFM), and wide-angle X-ray diffraction (WAXD). This study aims at unraveling the influence of the intralayer metal constituents of LDH on the crystallization rate, thermal stability, mechanical properties, and flame retardancy of iPP nanocomposites. It was found that iPP/LDH nanocomposites containing three-metal LDH showed better performance in thermal stability and flame retardancy compared to iPP/LDH nanocomposites containing two-metal LDH with the same loading.

RESULTS AND DISCUSSION

Characterization of LDH and Their Exfoliated Nanosheets. Both two-metal LDH (Co−Al and Zn−Al LDH) and three-metal LDH (Co−Zn−Al LDH) were synthesized under similar conditions by the co-precipitation method. The powder X-ray diffraction (XRD) patterns of LDH are displayed in Figure 1a. The sharp and symmetric features of the X-ray reflections corresponding to the (00n) planes suggest that the produced LDH have well-organized 2D layer stacking. A slight difference in the peak positions of (00n) planes of different LDH may be due to the presence of either different anions or number of water molecules within the LDH layer.[37,40] Several other reflections assigned to the lattice were observed in the 2θ range 30−70° (Figure S1). Overall, the X-ray pattern of the Co−Zn−Al LDH was nearly identical to those of Co−Al LDH and Zn−Al LDH in terms of peak positions and intensities. No peaks other than the typical LDH were detected, indicating the high purity of the obtained products. In the literature, a similar observation was made in the X-ray patterns of Mg−Al LDH upon the substitution of Mg^{2+} with Co^{2+} to obtain the Mg−Co−Al LDH.[41] Figure 1b shows the Fourier transform infrared spectroscopy (FTIR) spectra of the various LDH studied in this work. All LDH exhibited the characteristic bands for interlayer carbonate (CO_3^{2-}) and interlayer nitrate (NO_3^-) at 1356 and 1382 cm^{-1}, respectively. The conditions favoring the formation

DOI: 10.1021/acsomega.6b00485
ACS Omega 2017, 2, 20−31

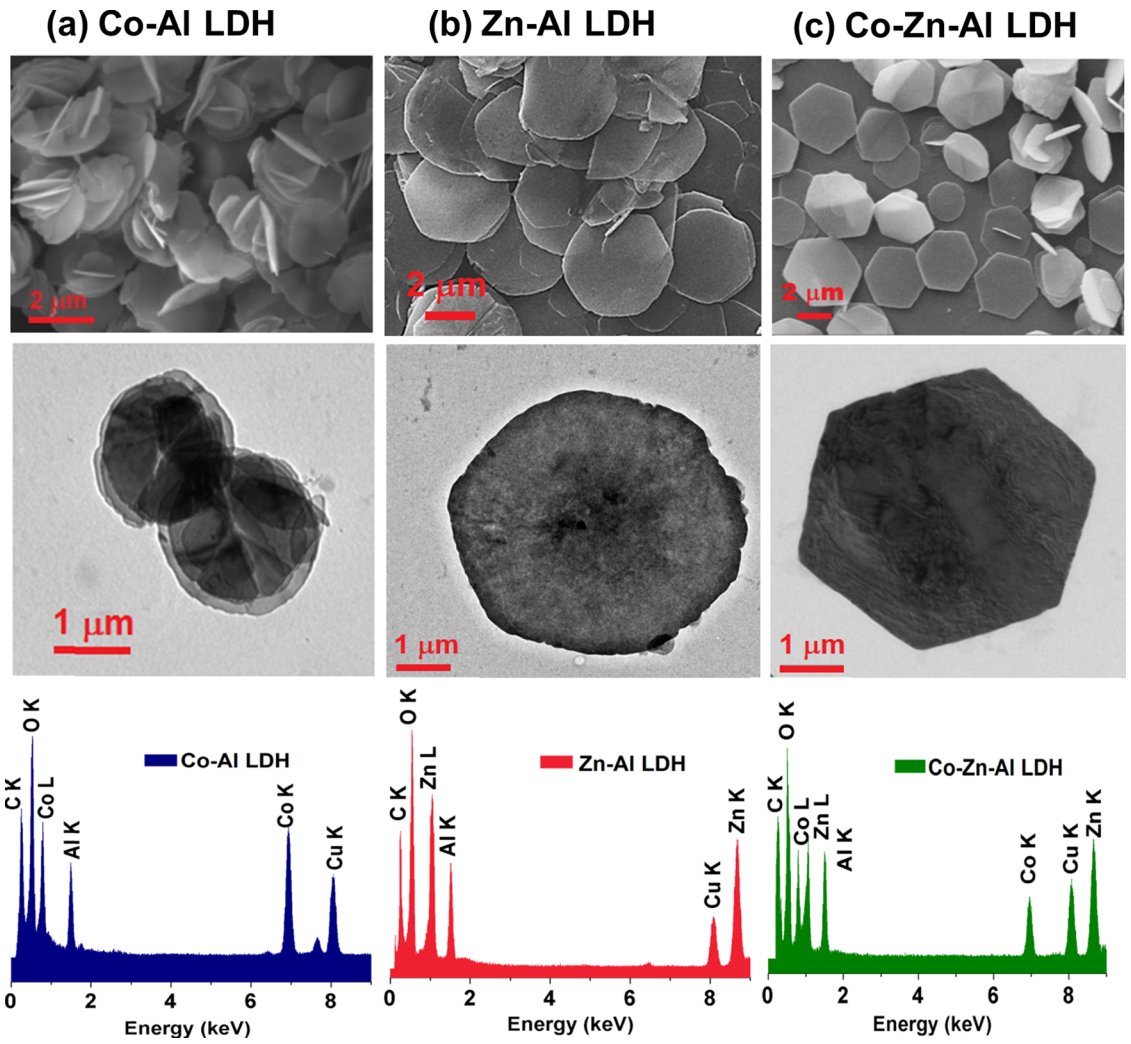

Figure 2. SEM, TEM, and EDS analysis of the as-synthesized LDH: (a) Co−Al LDH, (b) Zn−Al LDH, and (c) Co−Zn−Al LDH.

of CO_3^{2-} and NO_3^- were explained in our previous paper.[18] The presence of IR bands at 3440 cm^{-1} (ν (O-H)) and 1632 cm^{-1} (δ (H_2O)) confirmed the presence of interlayer water molecules.

To obtain the information about the size and shape of the as-synthesized LDH (bulk), the scanning electron microscopy (SEM) and TEM images were taken and are shown in Figure 2. The as-prepared LDH platelets displayed a three-dimensional (3D) platelet-like morphology with a dark contrast, indicating the presence of several layers of platelets in a single particle. However, the sizes and shapes of these LDH were found to be different from each other. The Co−Al LDH, Zn−Al LDH, and Co−Zn−Al LDH adopted different morphologies such as circular platelets, hexagonal platelets with rounded edges, and hexagonal platelets with sharp edges, respectively. This difference could be associated with the nucleation and growth mechanism of LDH in different reaction environments (metal salts) and conditions.[42] The chemical compositions of the different LDH were confirmed by energy-dispersive X-ray spectra (EDS) (Figure 2). The dominant oxygen peak in EDS of different LDH indicates the presence of water molecules within the layers as well as hydroxyl groups associated with the layers of the as-synthesized LDH platelets.

O'Hare and co-workers have recently reported an AMOST method for the preparation of stable dispersions of LDH in nonpolar solvents.[21,28] Recently, we have reported a slightly modified method to obtain highly delaminated sheets of LDH by sonication.[18] The advantage of this sonication process is simultaneous delamination and the lateral fragmentation of LDH. It is also worth mentioning here that ultrasonic vibration has been extensively used in the liquid exfoliation of 2D layered materials such as graphene, transition metal oxides, and transition metal dichalcogenides.[3,43−45] In this study, we used the same process to delaminate the different LDH in xylene. The SEM images of different LDH (Figure S2) show the broken platelets on a large scale, and the lateral size of LDH reduced to a few tens of nanometers. The ultrathin sheets of LDH were directly observed by TEM, as shown in Figure 3. It is evident that LDH platelets are broken into small pieces and exhibit a faint contrast compared to their bulk counterparts. Furthermore, high-resolution TEM was used to obtain more detailed information on the exfoliated LDH (Figure 3). These images revealed that the exfoliated LDH sheets are fairly clean and highly crystalline. The uniform atomic orientation and lattice spacing reveal that an individual layer consists of a single-crystal domain. The lattice fringes with the same *d*-spacings of ∼0.25 nm corresponding to the (012) crystal plane were observed in all LDH samples, and these values are consistent with the *d*-spacing estimated from the XRD results.[46] The EDS spectra of exfoliated LDH nanosheets are almost comparable to

DOI: 10.1021/acsomega.6b00485
ACS Omega 2017, 2, 20−31

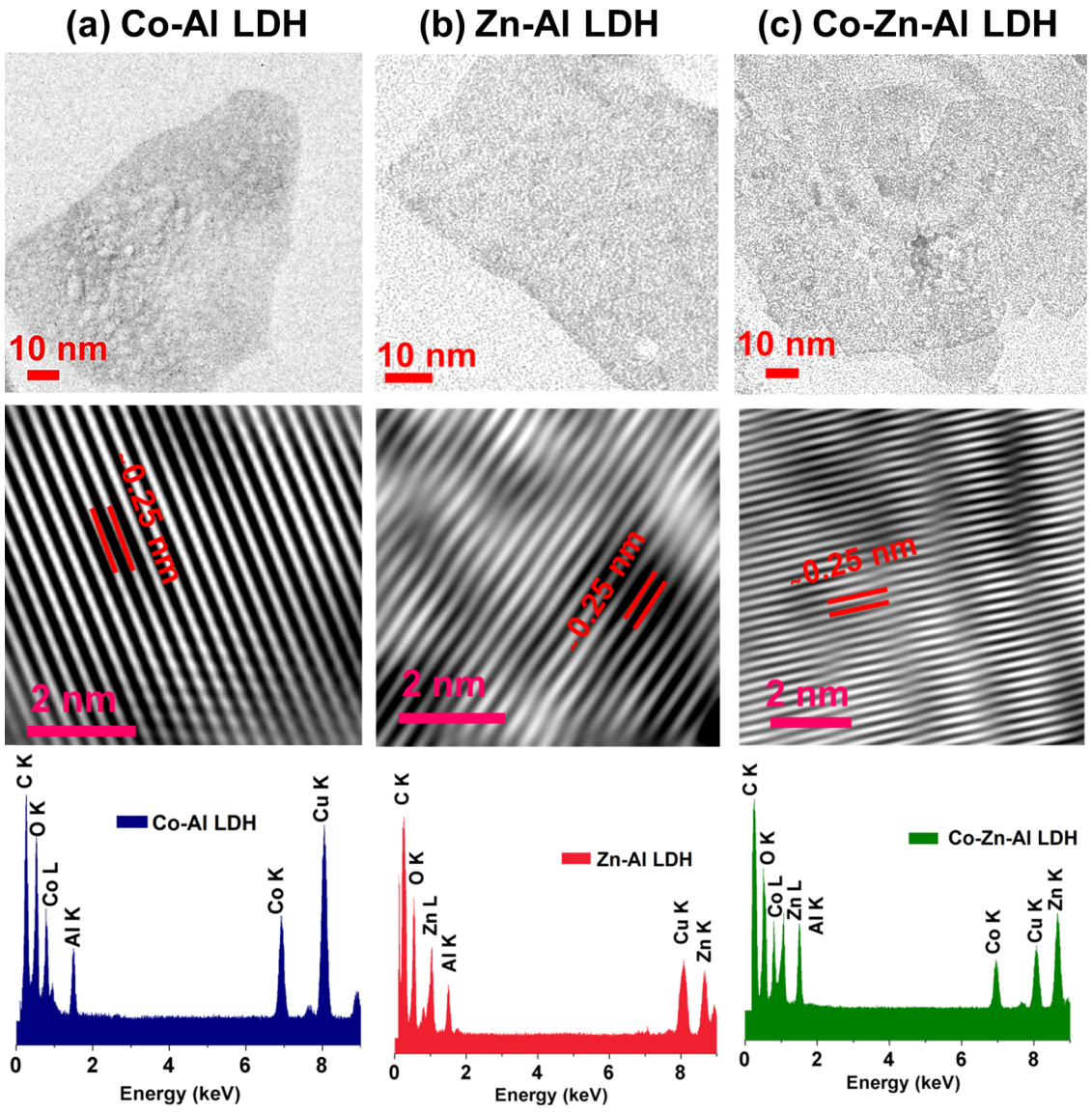

Figure 3. Low- and high-resolution TEM images and the corresponding energy-dispersive spectra of exfoliated LDH nanosheets: (a) Co−Al LDH, (b) Zn−Al LDH, and (c) Co−Zn−Al LDH.

those of their bulk counterparts other than the oxygen/carbon peak intensity ratio. The intensity of the oxygen peak decreased drastically, indicating the removal of water molecules in the exfoliated samples. The removal of water molecules in the exfoliated samples was further confirmed by FTIR spectra (data not shown here).

The thickness of Co−Zn−Al LDH (both in bulk and exfoliated form) was evaluated by AFM. Figure 4 shows the typical AFM height images and the corresponding height profiles of Co−Zn−Al LDH before and after exfoliation. It is evident from Figure 4a that the as-synthesized sample shows a 3D platelet-like morphology with lateral size ∼5 μm and thickness around a few hundreds of nanometers. On the other hand, the exfoliated nanosheets (Figure 4b) show that the thickness of the fragmented LDH is less than 1.0 nm. This value is in good agreement with the reported value for a single layer of LDH.[2,40] From these results, we may say that the as-synthesized sample contains a few hundreds of stacked layers of LDH. The lateral sizes of the exfoliated LDH range from 50 nm to a few hundreds of nanometers and are consistent with the TEM results.

Synthesis and Characterization of iPP/LDH Nanocomposites. Schematic representation of the methodology used for the preparation of highly dispersed iPP/LDH nanocomposites is shown in Figure 5. The as-synthesized LDH was washed with acetone to remove interlayer H_2O molecules from the stacked LDH layers. This process helps in converting the hydrophilic LDH to hydrophobic, and this facilitates the better dispersibility of LDH within the iPP matrix.[25,28] Subsequently, such washed LDH was sonicated for four days in xylene. The advantage of this step is the simultaneous surface modification and fragmentation of the LDH. Most importantly, this method produces 2D layered materials with lateral sizes and thickness in the nanometer range. The resultant LDH solution was directly added to the iPP solution to obtain highly dispersed nanocomposites. In this study, iPP nanocomposites were prepared using three different LDH (Co−Al LDH, Zn−Al LDH, and Co−Zn−Al LDH) by adjusting the amount of LDH to 6 wt %. In addition to this, to

DOI: 10.1021/acsomega.6b00485
ACS Omega 2017, 2, 20−31

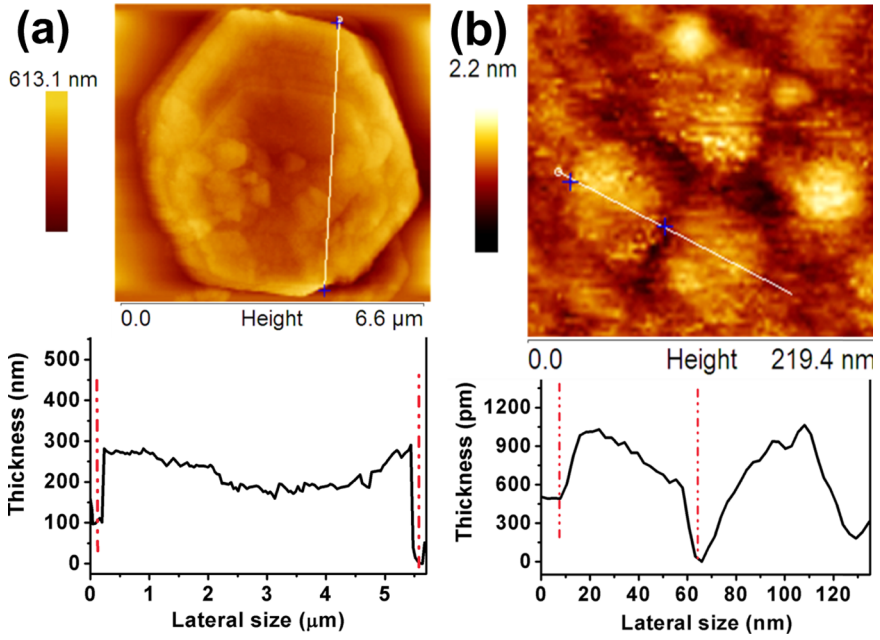

Figure 4. AFM images and height profiles of (a) as-synthesized and (b) exfoliated single-layer Co−Zn−Al LDH nanosheets.

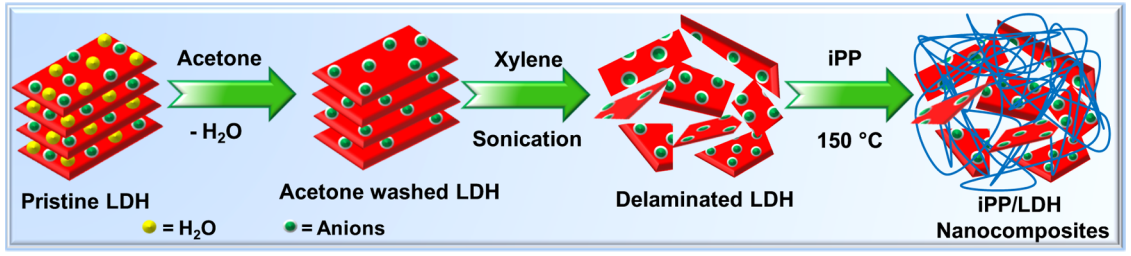

Figure 5. Schematic representation of the methodology used for the preparation of highly dispersed polymer nanocomposites based on iPP and LDHs.

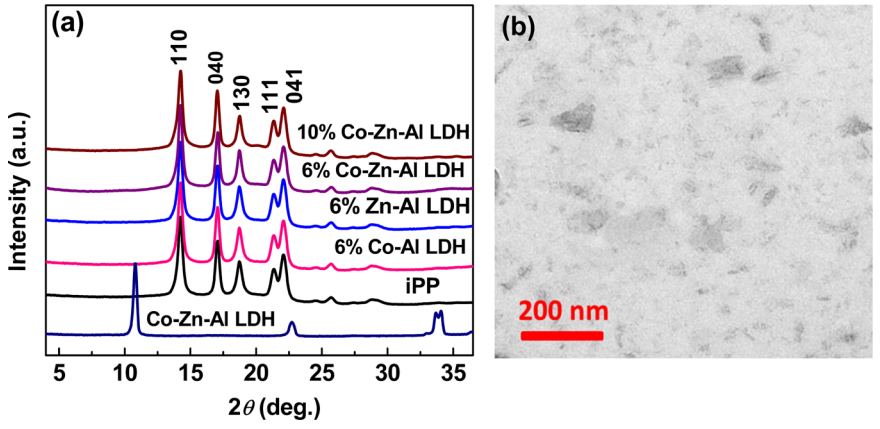

Figure 6. (a) Powder XRDs of iPP and its nanocomposites containing different types of LDH (for the purpose of comparison, the powder XRD pattern of LDH is shown) and (b) cross-sectional TEM image of the iPP/Co−Zn−Al LDH (10 wt %) nanocomposite.

understand the influence of LDH loading, in one case, iPP/LDH nanocomposites were prepared with 10 wt % of Co−Zn−Al LDH.

Such prepared iPP/LDH nanocomposites were crystallized isothermally at 130 °C after melting at 200 °C under strictly controlled conditions and analyzed by XRD. Figure 6a shows the XRD patterns of various nanocomposites along with pristine iPP and Co−Zn−Al LDH. The XRD patterns of nanocomposites are almost similar to those of pristine iPP. Both iPP and iPP/LDH nanocomposites show reflections corresponding to the monoclinic α form.[47] At the same time, no reflections corresponding to the $(00n)$ planes of LDH were observed in nanocomposites, indicating the loss of 2D layer stacking of LDH within the iPP matrix. These results suggest that exfoliated LDH platelets have been successfully dispersed into the polymer matrix without much agglomeration during

DOI: 10.1021/acsomega.6b00485
ACS Omega 2017, 2, 20−31

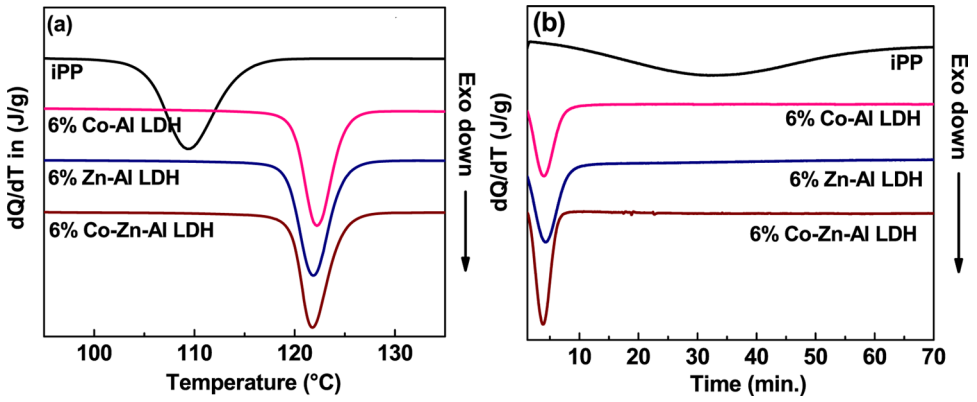

Figure 7. (a) DSC cooling thermograms of pristine iPP and its nanocomposites crystallized nonisothermally after melting at temperature 190 °C for 1 min. (b) Crystallization isotherms obtained at 132 °C for pristine iPP and its nanocomposites.

solution blending. The state of LDH dispersion within the iPP matrix was further confirmed by TEM measurements. Figure 6b shows a cross-sectional TEM image of the nanocomposite containing 10 wt % of Co−Zn−Al LDH. The nanosized LDH platelets are homogeneously dispersed in the polymer matrix with sizes ranging from 50 nm to a few hundreds of nanometers. This suggests that in the solution blending method LDH platelets are successfully transformed from solution to the solid state with minimum agglomeration.

Crystallization of iPP/LDH Nanocomposites. Tailoring the crystallinity and crystallization rate of semicrystalline polymers is of great importance to the polymer processing industry. The incorporation of nanofillers in polymer matrices is known to alter the crystallization behavior and the degree of crystallinity of the polymer matrix, which in turn controls the physical properties of the polymers.[18,48] To understand the effect of different LDH on the crystallization rate of iPP, the melt crystallization temperature (T_{mc}) was measured upon cooling the polymer melt. The T_{mc} values have often been used to measure the crystallization rate of the polymer. The higher the T_{mc}, the higher is the crystallization rate of the polymer.[49] Figure 7a shows differential scanning calorimetry (DSC) cooling curves of pristine iPP and its nanocomposites at 10 °C/min. Pristine iPP shows a T_{mc} at around 108 °C; however, the T_{mc} values shift to 121 ± 1 °C for nanocomposites irrespective of the type of LDH. The higher T_{mc} of the nanocomposites compared to that of iPP clearly indicates the faster crystallization of iPP in the presence of LDH; however, no change in the crystallization rate was observed with the type of LDH used for the preparation of nanocomposites.

To further confirm the effect of different types of LDH on the crystallization rate of iPP, the crystallization half-time ($T_{1/2}$) was obtained at an isothermal crystallization temperature (T_c). $T_{1/2}$ is usually defined as the time at which 50% of the crystallinity is developed. Figure 7b shows the representative DSC isothermal curves of pristine iPP and various nanocomposites crystallized at 132 °C. $T_{1/2}$ of pristine iPP was 33.3 min, and it decreased significantly for all nanocomposites irrespective of the type of LDH ($T_{1/2} \sim 4 \pm 0.2$ min). Usually, the crystallization rate G is the reciprocal of $T_{1/2}$, that is, $G = 1/T_{1/2}$. Figure 8 shows the temperature dependence of $1/T_{1/2}$ for pristine iPP and nanocomposites containing different types of LDH. It is observed that the crystallization rate decreases with increasing T_c for all of the samples, suggesting that the overall isothermal crystallization rate decreases with increasing T_c because of the low degree of supercooling ($\Delta T = T_m^\circ - T_c$,

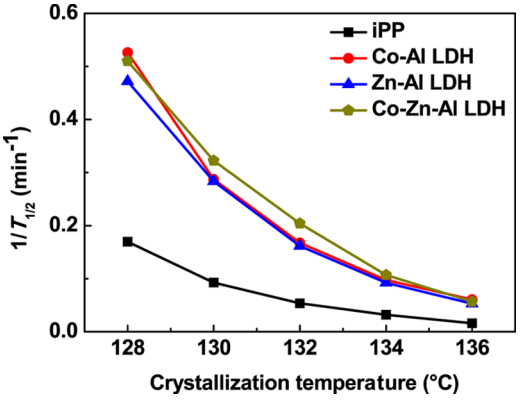

Figure 8. Temperature dependence of crystallization rate ($G = 1/T_{1/2}$) for pristine iPP and its nanocomposites using different types of LDH.

where T_m° is the equilibrium melting temperature) at higher T_c.[50] It was also observed that the crystallization rate of nanocomposites (0.53−0.05 min^{-1}) is higher than that of the pristine polymer (0.17−0.01 min^{-1}). These results suggested that the presence of LDH enhanced the crystallization process of iPP significantly, indicating that the fragmented LDH are effective nucleating agents for iPP. In our previous work, detailed crystallization kinetics has been carried out using different-sized LDH particles, and we showed that the lateral size of the LDH particles has a significant role in controlling the crystallization rate of iPP.[18] This study revealed that the type of LDH does not affect the crystallization rate of iPP.

Dynamic Mechanical Analysis (DMA). Inorganic fillers dispersed in a polymer matrix are known to influence the viscoelastic properties of the polymer.[51−53] The effect of the different types of LDH particles on the dynamic mechanical performance of iPP/LDH nanocomposites was investigated by DMA. Figure 9 shows the temperature dependence of the storage modulus (E') and loss tangent (tan δ) of iPP and its nanocomposites containing different types and amounts of LDH. Table 1 summarizes the DMA data extracted from Figure 9 for various samples. The storage modulus of pristine iPP is 2.5 GPa at −30 °C, and it decreases over the entire temperature range. The plateau region observed in the temperature range of −10 to 40 °C is associated with the relaxation of the amorphous region. The tan δ curve, which measures the energy dissipation (damping) ability of the material, shows peaks at 9.7 °C and another broad peak around ∼112 °C for pristine iPP. The first peak at 9.7 °C corresponds to the glass

DOI: 10.1021/acsomega.6b00485
ACS Omega 2017, 2, 20−31

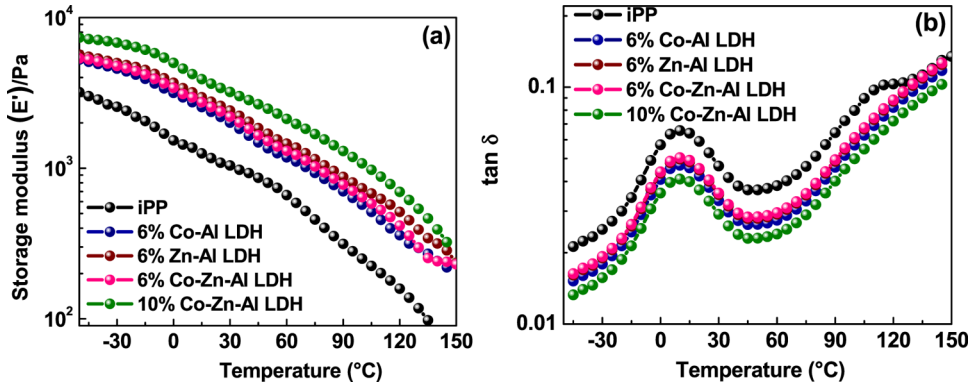

Figure 9. Temperature-dependent (a) storage modulus (E') and (b) loss factor (tan δ) measured in the heating process for iPP and its nanocomposites containing different LDH.

Table 1. Summary of the Degree of Crystallinity Measured from WAXD and Temperature-Dependent Dynamic Mechanical Properties

samples	X_c (%)[a] (±1)	E' at −30 °C (GPa) (±0.1)	E' at 30 °C (GPa) (±0.1)	E' at 100 °C (GPa) (±0.1)	tan δ_{max}(°C) (±1)
iPP	65.1	2.5	1.04	0.25	9.7
iPP/Co−Al LDH (6 wt %)	65.8	4.5	2.02	0.57	9.2
iPP/Zn−Al LDH (6 wt %)	65.8	4.6	2.46	0.70	9.6
iPP/Co−Zn−Al LDH (6 wt %)	64.6	4.65	2.2	0.64	10.3
iPP/Co−Zn−Al LDH (10 wt %)	63.3	6.580	3.25	1.08	9.8

[a]The degree of crystallinity (X_c) was calculated as the ratio of the area under the crystalline peaks to the total area under the X-ray scattering curve.

transition temperature (T_g), and the second one is attributed to the damping within the crystalline lamellae.[51−53] Around 150 °C, a sharp decrease in the storage modulus and a sudden increase in tan δ are due to the onset of melting of iPP crystals.

On addition of 6 wt % of different types of LDH, the storage modulus at −30 °C increased to 4.5, 4.6, and 4.65 GPa for nanocomposites containing Co−Al LDH, Zn−Al LDH, and Co−Zn−Al LDH, respectively, which is almost 1.8-fold increment compared to that of pristine iPP. The iPP/LDH nanocomposites exhibit a higher storage modulus across the measured temperature range. The average storage modulus measured at room temperature is almost two-fold higher for nanocomposites than that of pristine iPP. Increasing the LDH content to 10 wt % further increases the storage modulus to 6.6 and 3.2 GPa at −30 °C and room temperature, respectively, for iPP/Co−Zn−Al LDH nanocomposites. Generally, the increase in the storage modulus could be due to the increase in the percent crystallinity; however, in this present study, the percent of crystallinity (see Table 1) measured for various samples using the WAXD data shown in Figure 6 was almost the same for pristine iPP and iPP/LDH nanocomposites. Moreover, it is clearly observed that the increase in the LDH content increases the storage modulus of iPP. On the basis of these observations, the increase in the storage modulus could be attributed to the reinforcing effect of LDH, that is, the homogeneous dispersion of LDH within the polymer matrix without agglomerates. It has to be noted that a little or no difference in the storage modulus was observed with the type of LDH chosen (6 wt % loading) for the preparation of nanocomposites. The addition of LDH caused no change in the peak position of the tan δ curve near 9.5 °C, indicating that T_g of iPP did not change in the presence of the LDH particles. It is worth mentioning here that the T_g value of iPP is in the range −10 to 10 °C, depending on the grade and molecular weight.[51,54−56] However, the height of the tan δ peak decreases with the addition of LDH, which indicates the good wettability between the LDH and iPP.[51] In a few reports, it has been reported that T_g of the polymer was reduced, where the organically modified fillers were used for the preparation of nanocomposites due to the plasticization effect.[57] In some other cases, T_g of the polymer was increased due to the restricted mobility of the polymer chains in the presence of fillers.[51] However, in the present study, no change in T_g of iPP was observed in the presence of surfactant-free LDH particles. The magnitude of the broad peak around ∼112 °C, which was attributed to the damping within the crystalline lamellae, decreased for the nanocomposites. In nanocomposites, the LDH particles are expected to accumulate within the amorphous region of the polymer matrix. These particles influence the relaxation of iPP chains within the crystalline lamellae and crystalline−amorphous interfaces.

Flammability and Thermal Properties. Microscale combustion calorimetry (MCC) is a relatively new technique used for the evaluation of flammability of materials using small quantities of the sample, and this works on the principle of oxygen combustion. This technique was successfully used as a preliminary test for the evaluation of flame-retardant properties of polymer/LDH nanocomposites.[19,29−31] The heat release rate (HRR) is considered to be the most important parameter to estimate the flammability behavior of the polymer materials. Figure 10 presents the HRR plots for pristine iPP and its nanocomposites using different types and quantities of LDH. Several parameters such as the specific HRR, heat release capacity (HRC), and total heat release (THR) are summarized in Table 2 along with the 50% degradation temperature estimated from thermogravimetric analysis (TGA). Unlike the crystallization rate and storage modulus, the nanocomposites containing different types of LDH showed different HRR values. For pristine iPP, the HRR value is around 1435 W/g. With the addition of 6 wt % of different types of LDH, the HRR values were reduced to 1080, 990, and 880 W/g for Co−

DOI: 10.1021/acsomega.6b00485
ACS Omega 2017, 2, 20−31

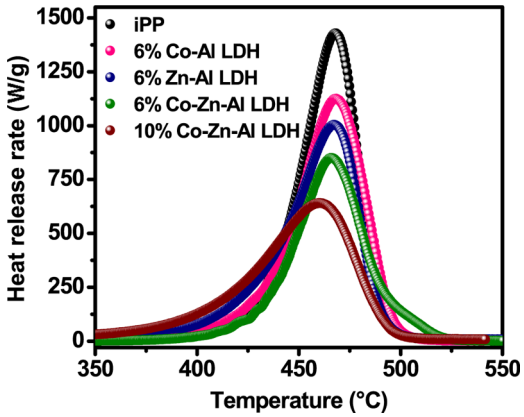

Figure 10. HRR vs temperature curves for pristine iPP and its nanocomposites containing Co−Al LDH (6 wt %), Zn−Al LDH (6 wt %), and Co−Zn−Al LDH (6 and 10 wt %).

Al LDH, Zn−Al LDH, and Co−Zn−Al LDH, respectively. These results clearly suggested that different LDH have different flame-retardant efficiencies. Three-metal LDH showed 38% reduction in the HRR value, which is better than that of the other two-metal LDH with the same LDH loadings. Matusinovic et al. showed that the dispersion of LDH in the polymer matrix is one of the key parameters in achieving good flame retardancy.[58] As discussed in the preceding section, highly dispersed nanocomposites were obtained using all types of LDH, so the dispersion of LDH may not be the key reason for the difference in the flame-retardant behavior. It was also demonstrated that different gallery anions have different flame-retardant efficiencies.[29,59,60] However, in the present study, the different LDH used have the same anions (both CO_3^{2-} and NO_3^-) because of the same protocol used for the synthesis of different LDH. It has been shown that the char formation can slow the HRR upon the ignition of polymers, and it can inhibit the flame spreading.[22,39,61,62] To understand the difference in the flame-retardant efficiency of different LDH, the amount of char formed upon the degradation of the polymer matrix was analyzed by TGA. Figure 11a shows the TGA thermograms of pristine iPP and its nanocomposites containing 6 wt % of different types of LDH. The thermal stability of the polymer is discussed in a later section. As seen from Figure 11a, the pristine polymer shows almost no char, whereas the samples containing different types of LDH show different char amounts ranging from 4.1 to 4.6 wt %. To further understand the reason for the difference in the char yield, TGA thermograms of different LDH were taken and are shown in Figure 11b. By considering the char yields of different LDH, the expected char residues were estimated for the nanocomposites prepared using different types of LDH and are shown in Table S1. It is quite clear that different LDH give different char yields, which follow the order Co−Zn−Al LDH > Zn−Al LDH > Co−Al LDH. Similar to char yields, the HRR also follows the same order. On the basis of these results, the lowest HRR value of the nanocomposite prepared using three-metal LDH (Co−Zn−Al LDH) can probably be attributed to the better char formation of three-metal LDH, which reduces the heat and mass transfer between the gas and condensed phases. It is worth mentioning here that LDH acts like both endothermic flame retardant and char forming flame retardant.[62] Under fire conditions, the LDH filler endothermically decomposes into water, carbon dioxide, metal hydroxides, and other gases, depending on the gallery anions. Furthermore, the decomposition products of the LDH are nonflammable, and so the residue left behind by the thermal decomposition (usually a metal oxide) dilutes the total amount of polymer fuel availability (condensed phase).[22] This process promotes the formation of char and protects the bulk polymer exposure to air. This char helps in reducing the HRR during the combustion and suppresses the smoke production. From the TGA results of LDH, it is clear that the char formation is effective in three-metal LDH compared to that of two-metal LDH.

To further verify the effect of LDH loading, 10 wt % of Co−Zn−Al LDH was added to iPP, and it was observed that the HRR value was further reduced by 55%. Wang and co-workers showed the reduction in the HRR value by 54% using 4 times higher LDH loadings (i.e., 40 wt %) in high-density polyethylene/LDH nanocomposites using MCC.[29] The HRC values estimated from the HRR curve (see Table 2) also show a similar trend like the HRR values, indicating that the three-metal LDH are efficient flame-retardant fillers compared to the two-metal LDH.

The THR calculated from the area under the HRR curve is an important parameter to understand the fire hazards of the material.[29,30] It has been shown that for an efficient flame-retardant filler, the THR value should reduce effectively when it is incorporated into the polymer.[29,30] It is obvious from Table 2 that the THR value is considerably reduced with the addition of 6 wt % of LDH and further reduced with increasing LDH loading to 10 wt %. A small difference in the THR values was observed with the type of LDH used for the preparation of nanocomposites. Three-metal LDH showed a lower THR value compared to that of the other two-metal LDH, indicating that the three-metal LDH is a better flame-retardant nanofiller for iPP.

The relative thermal stability of iPP was evaluated in the presence of different types of LDH. The 50% weight loss temperatures ($T_{0.5}$) measured for various samples from Figure 11a are summarized in Table 2. It can be seen that pristine iPP degraded completely with $T_{0.5}$ at 410 °C. The thermal decomposition temperature of iPP containing different types of LDH shifted to higher temperatures compared to pristine iPP. However, significant differences are seen in the thermal stability of nanocomposites containing different types of LDH. The $T_{0.5}$ values of iPP containing Co−Al LDH (6 wt %), Zn−

Table 2. Summary of Thermal and Flammability Properties for iPP and Its Nanocomposites

samples	HRR (W/g) (±5)	HRR reduction (%)	THR (kJ/g) (±1)	HRC (J/g K) (±5)	50% weight loss temperature (°C) (±2)
iPP	1435		54.0	1460	410
iPP/Co−Al LDH (6 wt %)	1080	25	49.9	1050	420
iPP/Zn−Al LDH (6 wt %)	990	31	48.7	985	430
iPP/Co−Zn−Al LDH (6 wt %)	880	39	48.17	905	443
iPP/Co−Zn−Al LDH (10 wt %)	640	55	43.9	690	435

DOI: 10.1021/acsomega.6b00485
ACS Omega 2017, 2, 20−31

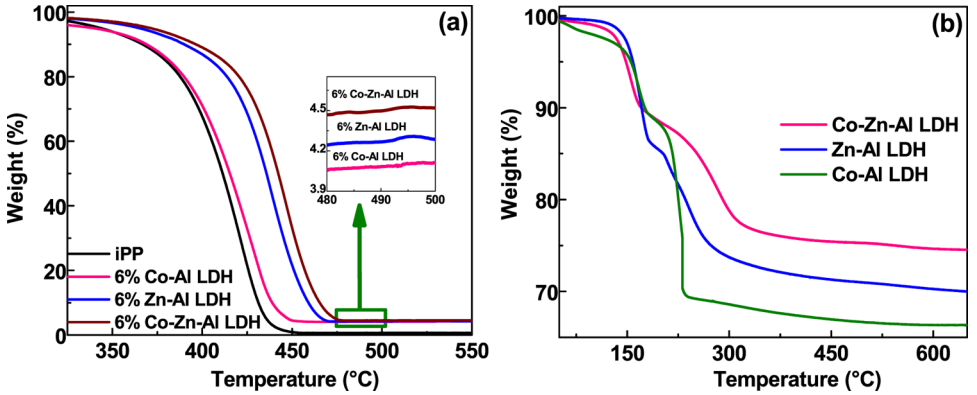

Figure 11. TGA thermograms for (a) pristine iPP and its nanocomposites containing 6 wt % of Co−Al LDH, Zn−Al LDH, and Co−Zn−Al LDH and for (b) pure LDH powders.

Al LDH (6 wt %), and Co−Zn−Al LDH (6 wt %) increased to 420, 430, and 443 °C, respectively. It has been shown that the enhanced thermal stability is due to the homogeneous dispersion of the nanosized LDH in the iPP matrix, where the dispersed nanoparticles act as trapping sites for the radicals generated during the degradation of the polymer.[18,21,23] However, in the present study, the dispersion of the LDH particles in the iPP matrix is more or less the same in different nanocomposites. One of the possibilities for the difference in the degradation temperature is the catalytic ability of the metal constituents used for the preparation of LDH. Typically, cobalt is known for the catalytic degradation of polyolefins.[63] However, in the present study, the cobalt containing three-metal LDH (Co−Zn−Al LDH) showed better thermal stability than the other two LDH. On the basis of the present results, we speculate that the difference in the thermal stability of iPP containing different types of LDH might be due to the thermally stable char formed by the degradation of LDH, which prevents further degradation of iPP. As mentioned in the preceding section, the char formation in different LDH follows the order Co−Zn−Al LDH > Zn−Al LDH > Co−Al LDH. Similar to this, the thermal stability and flame retardancy of the nanocomposites also follow the same order. On the other hand, the nanocomposite with 10 wt % of Co−Zn−Al LDH shows a $T_{0.5}$ value of ∼435 °C, which is less than the $T_{0.5}$ value of the nanocomposite containing 6 wt % of Co−Zn−Al LDH. This might be due to the agglomeration of LDH in higher loadings. Similar kinds of observations were reported in the literature.[18,23,28] It was shown that 2.5 wt % of sonicated LDH was the optimal loading for the effective thermal stability of iPP due to its better dispersion in the iPP matrix.[18] In this way, the intralayer metal constituents of LDH play an important role in determining the properties of the nanocomposites.

CONCLUSIONS

Two-metal LDH and three-metal LDH were successfully synthesized by the co-precipitation method and delaminated by ultrasonication in xylene. The sonication step resulted in both delamination and fragmentation of LDH. TEM and AFM analysis confirmed the delamination of LDH. Subsequently, highly dispersed iPP/LDH nanocomposites were prepared by the solution blending method. The dispersion of LDH within the iPP matrix was further confirmed by TEM and WAXD. We have found that the incorporation of either two-metal LDH or three-metal LDH dramatically improves the crystallization rate and storage modulus of iPP. However, not much difference is observed in these properties with the type of LDH used for the preparation of nanocomposites. On the other hand, the kind of LDH could influence the thermal stability and flame-retardant properties of iPP. Keeping the filler loading at 6 wt %, the 50% weight loss temperature ($T_{0.5}$) of the iPP nanocomposite containing three-metal LDH (Co−Zn−Al LDH) is higher than that of the corresponding nanocomposites prepared using the two-metal LDH (Co−Al LDH and Zn−Al LDH). Preliminary data on the flame-retardant properties showed better reduction in the HRR value compared to that of two-metal LDH containing nanocomposites. These differences might be due to the better char formation capability of three-metal LDH compared to that of two-metal LDH. These results demonstrated that the proper selection of metal constituents of LDH is imperative in the preparation of polymer/LDH nanocomposites with desirable properties.

EXPERIMENTAL SECTION

Materials. iPP pellets (M_w 120 000, M_w/M_n 4.5) were kindly supplied by Sumitomo Chemicals Co. Ltd., Japan. Metal salts such as $Al(NO_3)_3{\cdot}9H_2O$, $Co(NO_3)_2{\cdot}6H_2O$, and $Zn(NO_3)_2{\cdot}6H_2O$ were purchased from Sigma-Aldrich Co. Ltd. Other chemicals such as urea, xylene, ethanol, and acetone were obtained from Merck, India.

Synthesis of LDH. Different types of LDH used in this study were synthesized by a conventional co-precipitation method using urea as the base. Three-metal LDH (Co−Zn−Al LDH) was prepared by dissolving three metal salts ($Co(NO_3)_2{\cdot}6H_2O$, $Zn(NO_3)_2{\cdot}6H_2O$, and $Al(NO_3)_3{\cdot}9H_2O$), and urea in Millipore water with a ratio of 1:1:1:7. The total mixture was then heated to the refluxing temperature (about 100 °C) under continuous stirring for 24 h in an ambient atmospheric environment. The resultant light pink color precipitate was rapidly quenched in cold water and filtered, and then the precipitate was repeatedly washed with hot Millipore water to remove the unreacted reactants if any. The thus-obtained LDH powder was repeatedly washed with acetone. The end product was dispersed in xylene and sonicated for 4 days in an ultrasonication bath at room temperature. The resulting suspension was stable at room temperature for a few hours. Two-metal LDH (Co−Al LDH and Zn−Al LDH) were synthesized in the same way, with the exception that the Co^{2+} and Al^{3+}, Zn^{2+} and Al^{3+} metal nitrates were taken in 2:1 ratio.

Preparation of iPP/LDH Nanocomposites. Three different LDH (Co−Zn−Al LDH, Co−Al LDH, and Zn−Al LDH)

DOI: 10.1021/acsomega.6b00485
ACS Omega 2017, 2, 20−31

were used as reinforcement fillers for the preparation of iPP nanocomposites. The synthetic procedure is as follows: for example, to prepare 6 wt % of iPP/LDH nanocomposite, 0.06 g of LDH powder was dispersed in 150 mL of xylene in an ultrasonic bath for four days at 45 °C to yield a uniform suspension. Then, 0.94 g of iPP was dissolved in the suspension and the sonication was continued for 10 min. The resultant solution was refluxed at 150 °C with continuous magnetic stirring for 24 h under an argon atmosphere. Finally, the polymer solution was reprecipitated out in ethanol. The precipitate was filtrated, washed with ethanol, and vacuum dried at 100 °C for 24 h. The type and amount of LDH were adjusted to prepare different nanocomposites with various LDH loadings (0, 6, and 10%). The actual loading of the LDH in iPP was estimated using TGA and the details are given in Table S1.

Characterization. *WAXD.* XEUSS 2D SAXS/WAXS system with a Genix microsource from Xenocs was used for the WAXD measurements. The X-ray system was operated at 50 kV and 0.6 mA. The Cu Kα radiation (λ = 1.54 Å) was collimated with a FOX2D mirror and two pairs of scatterless slits. The measurements were carried out in the transmission geometry. The fiber diagrams were recorded on a Mar345 image plate and processed using the Fit2D software. The sample to the detector distance was 214.5 mm. Samples were crystallized under controlled conditions using a differential scanning calorimeter, and the prepared samples were used for the XRD measurements.

FTIR. A Perkin Elmer Series FTIR spectrum-2 was used to measure the infrared spectrum over the wavenumber range 4000−400 cm^{-1}. The dried LDH powder was mixed with KBr and pressed in the form of pellets for FTIR measurements. The spectra were collected with 32 scans and a resolution of 1 cm^{-1}.

SEM. The shape and size of the LDH were investigated by SEM (Zeiss EVO 18 cryo-SEM) with an accelerating voltage of 20 kV. LDH suspension was directly drop-cast onto a carbon-coated grid and imaged after natural drying at room temperature. Before imaging, a thin layer of gold was evaporated onto the sample to avoid charging and to improve contrast.

TEM. A JEOL 2010 transmission electron microscope operating at 300 kV was used to investigate the LDH morphology. LDH suspension was directly drop-cast on a carbon-coated copper grid and allowed for natural drying for two days in a dust-free environment. The prepared samples were then used for both imaging and elemental composition analysis using an energy-dispersive spectrometer (Technai G^2 30LaB_6, ST with EDS). To view the dispersion of LDH in the polymer matrix, ultrathin sections of the nanocomposite samples (∼ 60 nm thickness) were sliced with a diamond knife (35° knife angle; DIATOME, Switzerland) using ultramicrotome EM UC/FC 6, Leica (Austria) at −140 °C. The sections were floated with a dimethyl sulfoxide/water mixture on a carbon-filmed TEM copper grid. These thin slices of the samples were analyzed using a TEM LIBRA 120, Carl Zeiss Microscopy GmbH (Oberkochen, Germany), with an acceleration voltage of 120 kV.

AFM. The surface morphology and thickness of the LDH sheets were analyzed using a Bruker Multimode atomic force microscope, Germany, in the tapping mode. The as-synthesized LDH in water and the sonicated LDH suspension in xylene were coated on silicon wafers.

TGA. TGA thermograms were collected in the heating process at 10 °C/min using TA Q50. All measurements were carried out under a nitrogen atmosphere (nitrogen gas flow rate of 60 mL/min for the furnace and 40 mL/min for the balance).

DSC. DSC measurements were performed on a Perkin Elmer Pyris 6 DSC apparatus under nitrogen gas flow. The temperature and heat flow were calibrated using high-purity indium. The crystallization half-time ($T_{1/2}$) was measured to evaluate the crystallization rate of iPP and its nanocomposites. Molten samples were rapidly cooled to the desired crystallization temperature (T_c) (132 °C) at a rate of 100 °C/min, and the samples were allowed to crystallize at that temperature. These samples were reheated to 190 °C to measure the melting temperature.

MCC. The MCC-1 (FTT) was used as a preliminary test to evaluate the combustion behavior of iPP and iPP/LDH nanocomposites. In the MCC system, approximately 5 mg of the sample was heated to 700 °C at a heating rate of 1 °C/s in a stream of N_2 flow at 80 cm^3/min. The resulting volatile anaerobic thermal degradation products in the nitrogen gas stream are mixed with 80 cm^3/min carrying gas (nitrogen of 80 mL/min; oxygen of 20 mL/min) and subsequently burned at 900 °C in a combustion furnace. The flame-retardant parameters were measured from this test, and are the HRR in W/g, % of reduction in HRR, THR rate in KJ/g, temperature maxima (T_{max}) in °C, and HRC in J/g K.

DMA. DMA (TA Instruments Model Q800) was used to study the temperature-dependent dynamic mechanical properties of the samples. The samples with dimensions 25 × 6 × 0.4 mm^3 were prepared using the hot press. All samples were annealed at 130 °C for 5 h. The prepared samples were used to measure the temperature-dependent storage modulus (E'), loss modulus (E''), and their ratio (tan δ) at a constant frequency (ω) of 6.28 rad/s with a strain amplitude of 0.05%. The measurements were carried out in a temperature range of −50 to 160 °C, with a heating rate of 2 °C/min.

■ ASSOCIATED CONTENT

Supporting Information

The Supporting Information is available free of charge on the ACS Publications website at DOI: 10.1021/acsomega.6b00485.

Powder XRD patterns of (a) Co−Zn−Al LDH, (b) pristine iPP, and (c) iPP/Co−Zn−Al LDH nanocomposites (Figure S1); SEM images of fragmented LDH nanosheets (a) Co−Al LDH, (b) Zn−Al LDH, and (c) Co−Zn−Al LDH (Figure S2); summary of char yields of the as-synthesized LDH and its nanocomposites (Table S1) (PDF)

■ AUTHOR INFORMATION

Corresponding Author

*E-mail: bhojegowd@niist.res.in. Tel: +91-471-2515474. Fax: +91-471-2491712.

Notes

The authors declare no competing financial interest.

■ ACKNOWLEDGMENTS

The authors thank Dr. P. Prabhakar Rao, Kiran Mohan, and Dr. Yoosaf Karuvath and Aswin CSIR-NIIST for extending the SEM, TEM, and AFM facilities, respectively. The authors also thank Prof. Tushar Jana, University of Hyderabad, for DMA measurements and Dr. Petr Formanek, IPF, Dresden, Germany,

DOI: 10.1021/acsomega.6b00485
ACS Omega 2017, 2, 20−31

for TEM analysis of polymer nanocomposites. E.B.G. thanks the Department of Science and Technology (Government of India) for the research project vide No.: SB/S3/CE/070/2014. The authors also thank the Council of Scientific and Industrial Research, India, for financial support in the form of 12th FYP project (CSC-0135). B.N. thanks the Council of Scientific and Industrial Research for the award of a research fellowship.

REFERENCES

(1) Geim, A. K. Graphene: Status and Prospects. *Science* **2009**, *324*, 1530−1534.
(2) Liu, Z.; Ma, R.; Osada, M.; Iyi, N.; Ebina, Y.; Takada, K.; Sasaki, T. Synthesis, Anion Exchange, and Delamination of Co−Al Layered Double Hydroxide: Assembly of the Exfoliated Nanosheet/Polyanion Composite Films and Magneto-Optical Studies. *J. Am. Chem. Soc.* **2006**, *128*, 4872−4880.
(3) Coleman, J. N.; Lotya, M.; O'Neill, A.; Bergin, S. D.; King, P. J.; Khan, U.; Young, K.; Gaucher, A.; De, S.; Smith, R. J.; Shvets, I. V.; Arora, S. K.; Stanton, G.; Kim, H.-Y.; Lee, K.; Kim, G. T.; Duesberg, G. S.; Hallam, T.; Boland, J. J.; Wang, J. J.; Donegan, J. F.; Grunlan, J. C.; Moriarty, G.; Shmeliov, A.; Nicholls, R. J.; Perkins, J. M.; Grieveson, E. M.; Theuwissen, K.; McComb, D. W.; Nellist, P. D.; Nicolosi, V. Two-Dimensional Nanosheets Produced by Liquid Exfoliation of Layered Materials. *Science* **2011**, *331*, 568−571.
(4) Naik, V. V.; Ramesh, T. N.; Vasudevan, S. Neutral Nanosheets that Gel: Exfoliated Layered Double Hydroxides in Toluene. *J. Phys. Chem. Lett.* **2011**, *2*, 1193−1198.
(5) Novoselov, K. S.; Geim, A. K.; Morozov, S. V.; Jiang, D.; Zhang, Y.; Dubonos, S. V.; Grigorieva, I. V.; Firsov, A. A. Electric Field Effect in Atomically Thin Carbon Films. *Science* **2004**, *306*, 666−669.
(6) Nicolosi, V.; Chhowalla, M.; Kanatzidis, M. G.; Strano, M. S.; Coleman, J. N. Liquid Exfoliation of Layered Materials. *Science* **2013**, *340*, 1420.
(7) Wang, D.-Y.; Das, A.; Leuteritz, A.; Mahaling, R. N.; Jehnichen, D.; Wagenknecht, U.; Heinrich, G. Structural characteristics and flammability of fire retarding EPDM/layered double hydroxide (LDH) nanocomposites. *RSC Adv.* **2012**, *2*, 3927−3933.
(8) Alexandre, M.; Dubois, P. Polymer-layered silicate nanocomposites: preparation, properties and uses of a new class of materials. *Mater. Sci. Eng., R* **2000**, *28*, 1−63.
(9) Song, W.-L.; Wang, P.; Cao, L.; Anderson, A.; Meziani, M. J.; Farr, A. J.; Sun, Y.-P. Polymer/Boron Nitride Nanocomposite Materials for Superior Thermal Transport Performance. *Angew. Chem., Int. Ed.* **2012**, *51*, 6498−6501.
(10) Novoselov, K. S.; Jiang, D.; Schedin, F.; Booth, T. J.; Khotkevich, V. V.; Morozov, S. V.; Geim, A. K. Two-dimensional atomic crystals. *Proc. Natl. Acad. Sci. U.S.A.* **2005**, *102*, 10451−10453.
(11) Zhang, Y.; Zhang, L.; Zhou, C. Review of Chemical Vapor Deposition of Graphene and Related Applications. *Acc. Chem. Res.* **2013**, *46*, 2329−2339.
(12) Paul, D. R.; Robeson, L. M. Polymer nanotechnology: Nanocomposites. *Polymer* **2008**, *49*, 3187−3204.
(13) Spitalsky, Z.; Tasis, D.; Papagelis, K.; Galiotis, C. Carbon nanotube−polymer composites: Chemistry, processing, mechanical and electrical properties. *Prog. Polym. Sci.* **2010**, *35*, 357−401.
(14) Kim, H.; Abdala, A. A.; Macosko, C. W. Graphene/Polymer Nanocomposites. *Macromolecules* **2010**, *43*, 6515−6530.
(15) Leroux, F.; Besse, J.-P. Polymer Interleaved Layered Double Hydroxide: A New Emerging Class of Nanocomposites. *Chem. Mater.* **2001**, *13*, 3507−3515.
(16) Basu, D.; Das, A.; Stöckelhuber, K. W.; Wagenknecht, U.; Heinrich, G. Advances in layered double hydroxide (LDH)-based elastomer composites. *Prog. Polym. Sci.* **2014**, *39*, 594−626.
(17) Gao, Y.; Wu, J.; Wang, Q.; Wilkie, C. A.; O'Hare, D. Flame retardant polymer/layered double hydroxide nanocomposites. *J. Mater. Chem. A* **2014**, *2*, 10996−11016.
(18) Nagendra, B.; Mohan, K.; Gowd, E. B. Polypropylene/Layered Double Hydroxide (LDH) Nanocomposites: Influence of LDH Particle Size on the Crystallization Behavior of Polypropylene. *ACS Appl. Mater. Interfaces* **2015**, *7*, 12399−12410.
(19) Nagendra, B.; Das, A.; Leuteritz, A.; Gowd, E. B. Structure and crystallization behaviour of syndiotactic polystyrene/layered double hydroxide nanocomposites. *Polym. Int.* **2016**, *65*, 299−307.
(20) Chen, W.; Qu, B. LLDPE/ZnAl LDH-exfoliated nanocomposites: effects of nanolayers on thermal and mechanical properties. *J. Mater. Chem.* **2004**, *14*, 1705−1710.
(21) Wang, Q.; Zhang, X.; Zhu, J.; Guo, Z.; O'Hare, D. Preparation of stable dispersions of layered double hydroxides (LDHs) in nonpolar hydrocarbons: new routes to polyolefin/LDH nanocomposites. *Chem. Commun.* **2012**, *48*, 7450−7452.
(22) Matusinovic, Z.; Wilkie, C. A. Fire retardancy and morphology of layered double hydroxide nanocomposites: a review. *J. Mater. Chem.* **2012**, *22*, 18701−18704.
(23) Wang, Q.; Zhang, X.; Wang, C. J.; Zhu, J.; Guo, Z.; O'Hare, D. Polypropylene/layered double hydroxide nanocomposites. *J. Mater. Chem.* **2012**, *22*, 19113−19121.
(24) Yang, J.-H.; Zhang, W.; Ryu, H.; Lee, J.-H.; Park, D.-H.; Choi, J. Y.; Vinu, A.; Elzatahry, A. A.; Choy, J.-H. Influence of anionic surface modifiers on the thermal stability and mechanical properties of layered double hydroxide/polypropylene nanocomposites. *J. Mater. Chem. A* **2015**, *3*, 22730−22738.
(25) O'Leary, S.; O'Hare, D.; Seeley, G. Delamination of layered double hydroxides in polar monomers: new LDH-acrylate nanocomposites. *Chem. Commun.* **2002**, 1506−1507.
(26) Chen, W.; Qu, B. Structural Characteristics and Thermal Properties of PE-g-MA/MgAl-LDH Exfoliation Nanocomposites Synthesized by Solution Intercalation. *Chem. Mater.* **2003**, *15*, 3208−3213.
(27) Chen, W.; Feng, L.; Qu, B. Preparation of Nanocomposites by Exfoliation of ZnAl Layered Double Hydroxides in Nonpolar LLDPE Solution. *Chem. Mater.* **2004**, *16*, 368−370.
(28) Wang, Q.; Undrell, J. P.; Gao, Y.; Cai, G.; Buffet, J.-C.; Wilkie, C. A.; O'Hare, D. Synthesis of Flame-Retardant Polypropylene/LDH-Borate Nanocomposites. *Macromolecules* **2013**, *46*, 6145−6150.
(29) Gao, Y.; Wang, Q.; Wang, J.; Huang, L.; Yan, X.; Zhang, X.; He, Q.; Xing, Z.; Guo, Z. Synthesis of Highly Efficient Flame Retardant High-Density Polyethylene Nanocomposites with Inorgano-Layered Double Hydroxides As Nanofiller Using Solvent Mixing Method. *ACS Appl. Mater. Interfaces* **2014**, *6*, 5094−5104.
(30) Wang, D.-Y.; Das, A.; Costa, F. R.; Leuteritz, A.; Wang, Y.-Z.; Wagenknecht, U.; Heinrich, G. Synthesis of Organo Cobalt−Aluminum Layered Double Hydroxide via a Novel Single-Step Self-Assembling Method and Its Use as Flame Retardant Nanofiller in PP. *Langmuir* **2010**, *26*, 14162−14169.
(31) Kang, N.-J.; Wang, D.-Y.; Kutlu, B.; Zhao, P.-C.; Leuteritz, A.; Wagenknecht, U.; Heinrich, G. A New Approach to Reducing the Flammability of Layered Double Hydroxide (LDH)-Based Polymer Composites: Preparation and Characterization of Dye Structure-Intercalated LDH and Its Effect on the Flammability of Polypropylene-Grafted Maleic Anhydride/D-LDH Composites. *ACS Appl. Mater. Interfaces* **2013**, *5*, 8991−8997.
(32) Purohit, P. J.; Huacuja-Sánchez, J. E.; Wang, D.-Y.; Emmerling, F.; Thünemann, A.; Heinrich, G.; Schönhals, A. Structure−Property Relationships of Nanocomposites Based on Polypropylene and Layered Double Hydroxides. *Macromolecules* **2011**, *44*, 4342−4354.
(33) Wang, Q.; Tay, H. H.; Ng, D. J. W.; Chen, L.; Liu, Y.; Chang, J.; Zhong, Z.; Luo, J.; Borgna, A. The Effect of Trivalent Cations on the Performance of Mg-M-CO_3 Layered Double Hydroxides for High-Temperature CO_2 Capture. *ChemSusChem* **2010**, *3*, 965−973.
(34) Zhao, Y.; Wei, M.; Lu, J.; Wang, Z. L.; Duan, X. Biotemplated Hierarchical Nanostructure of Layered Double Hydroxides with Improved Photocatalysis Performance. *ACS Nano* **2009**, *3*, 4009−4016.
(35) Yang, M.; McDermott, O.; Buffet, J.-C.; O'Hare, D. Synthesis and characterisation of layered double hydroxide dispersions in organic solvents. *RSC Adv.* **2014**, *4*, 51676−51682.

DOI: 10.1021/acsomega.6b00485
ACS Omega 2017, 2, 20−31

(36) Wang, Q.; O'Hare, D. Large-scale synthesis of highly dispersed layered double hydroxide powders containing delaminated single layer nanosheets. *Chem. Commun.* **2013**, *49*, 6301−6303.
(37) Gao, Y.; Wu, J.; Zhang, Z.; Jin, R.; Zhang, X.; Yan, X.; Umar, A.; Guo, Z.; Wang, Q. Synthesis of polypropylene/Mg_3Al-X (X = CO_3^{2-}, NO_3^-, Cl^-, SO_4^{2-}) LDH nanocomposites using a solvent mixing method: thermal and melt rheological properties. *J. Mater. Chem. A* **2013**, *1*, 9928−9934.
(38) Qiu, L.; Gao, Y.; Yan, X.; Guo, J.; Umar, A.; Guo, Z.; Wang, Q. Morphology-dependent performance of Mg_3Al-CO_3 layered double hydroxide as a nanofiller for polypropylene nanocomposites. *RSC Adv.* **2015**, *5*, 51900−51911.
(39) Wang, X.; Sporer, Y.; Leuteritz, A.; Kuehnert, I.; Wagenknecht, U.; Heinrich, G.; Wang, D.-Y. Comparative study of the synergistic effect of binary and ternary LDH with intumescent flame retardant on the properties of polypropylene composites. *RSC Adv.* **2015**, *5*, 78979−78985.
(40) Song, F.; Hu, X. Exfoliation of layered double hydroxides for enhanced oxygen evolution catalysis. *Nat. Commun.* **2014**, *5*, 4477.
(41) Kim, T.-H.; Lee, W.-J.; Lee, J.-Y.; Paek, S.-M.; Oh, J.-M. Isomorphous substitution of divalent metal ions in layered double hydroxides through a soft chemical hydrothermal reaction. *Dalton Trans.* **2014**, *43*, 10430−10437.
(42) Yokoi, T.; Tsukada, K.; Terasaka, S.; Kamitakahara, M.; Matsubara, H. Morphological control of layered double hydroxide through a biomimetic approach using carboxylic and sulfonic acids. *J. Asian Ceram. Soc.* **2015**, *3*, 230−233.
(43) Ciesielski, A.; Samori, P. Graphene via sonication assisted liquid-phase exfoliation. *Chem. Soc. Rev.* **2014**, *43*, 381−398.
(44) Han, J. T.; Jang, J. I.; Kim, H.; Hwang, J. Y.; Yoo, H. K.; Woo, J. S.; Choi, S.; Kim, H. Y.; Jeong, H. J.; Jeong, S. Y.; Baeg, K.-J.; Cho, K.; Lee, G.-W. Extremely Efficient Liquid Exfoliation and Dispersion of Layered Materials by Unusual Acoustic Cavitation. *Sci. Rep.* **2014**, *4*, 5133.
(45) Chhowalla, M.; Shin, H. S.; Eda, G.; Li, L.-J.; Loh, K. P.; Zhang, H. The chemistry of two-dimensional layered transition metal dichalcogenide nanosheets. *Nat. Chem.* **2013**, *5*, 263−275.
(46) Zhao, Y.; Chen, G.; Bian, T.; Zhou, C.; Waterhouse, G. I. N.; Wu, L.-Z.; Tung, C.-H.; Smith, L. J.; O'Hare, D.; Zhang, T. Defect-Rich Ultrathin ZnAl-Layered Double Hydroxide Nanosheets for Efficient Photoreduction of CO_2 to CO with Water. *Adv. Mater.* **2015**, *27*, 7824−7831.
(47) Jones, A. T.; Aizlewood, J. M.; Beckett, D. R. Crystalline forms of isotactic polypropylene. *Makromol. Chem.* **1964**, *75*, 134−158.
(48) Fornes, T. D.; Paul, D. R. Crystallization behavior of nylon 6 nanocomposites. *Polymer* **2003**, *44*, 3945−3961.
(49) Mani, M. R.; Chellaswamy, R.; Marathe, Y. N.; Pillai, V. K. The role of the molecular structure of carboxylate-alumoxanes in the enhanced nucleation of polypropylene. *Chem. Commun.* **2015**, *51*, 10026−10029.
(50) Qiu, Z.; Li, Z. Effect of Orotic Acid on the Crystallization Kinetics and Morphology of Biodegradable Poly(l-lactide) as an Efficient Nucleating Agent. *Ind. Eng. Chem. Res.* **2011**, *50*, 12299−12303.
(51) Díez-Pascual, A. M.; Naffakh, M. Polypropylene/Glass Fiber Hierarchical Composites Incorporating Inorganic Fullerene-like Nanoparticles for Advanced Technological Applications. *ACS Appl. Mater. Interfaces* **2013**, *5*, 9691−9700.
(52) Liu, P.; White, K. L.; Sugiyama, H.; Xi, J.; Higuchi, T.; Hoshino, T.; Ishige, R.; Jinnai, H.; Takahara, A.; Sue, H.-J. Influence of Trace Amount of Well-Dispersed Carbon Nanotubes on Structural Development and Tensile Properties of Polypropylene. *Macromolecules* **2013**, *46*, 463−473.
(53) Maiti, P.; Nam, P. H.; Okamoto, M.; Hasegawa, N.; Usuki, A. Influence of Crystallization on Intercalation, Morphology, and Mechanical Properties of Polypropylene/Clay Nanocomposites. *Macromolecules* **2002**, *35*, 2042−2049.
(54) Naffakh, M.; Remskar, M.; Marco, C.; Gomez-Fatou, M. A.; Jimenez, I. Towards a new generation of polymer nanocomposites based on inorganic nanotubes. *J. Mater. Chem.* **2011**, *21*, 3574−3578.
(55) Nam, P. H.; Maiti, P.; Okamoto, M.; Kotaka, T.; Hasegawa, N.; Usuki, A. A hierarchical structure and properties of intercalated polypropylene/clay nanocomposites. *Polymer* **2001**, *42*, 9633−9640.
(56) Leelapornpisit, W.; Ton-That, M.-T.; Perrin-Sarazin, F.; Cole, K. C.; Denault, J.; Simard, B. Effect of carbon nanotubes on the crystallization and properties of polypropylene. *J. Polym. Sci., Part B: Polym. Phys.* **2005**, *43*, 2445−2453.
(57) Wang, K.; Liang, S.; Deng, J.; Yang, H.; Zhang, Q.; Fu, Q.; Dong, X.; Wang, D.; Han, C. C. The role of clay network on macromolecular chain mobility and relaxation in isotactic polypropylene/organoclay nanocomposites. *Polymer* **2006**, *47*, 7131−7144.
(58) Matusinovic, Z.; Feng, J.; Wilkie, C. A. The role of dispersion of LDH in fire retardancy: The effect of different divalent metals in benzoic acid modified LDH on dispersion and fire retardant properties of polystyrene− and poly(methyl-methacrylate)−LDH−B nanocomposites. *Polym. Degrad. Stab.* **2013**, *98*, 1515−1525.
(59) Nyambo, C.; Songtipya, P.; Manias, E.; Jimenez-Gasco, M. M.; Wilkie, C. A. Effect of MgAl-layered double hydroxide exchanged with linear alkyl carboxylates on fire-retardancy of PMMA and PS. *J. Mater. Chem.* **2008**, *18*, 4827−4838.
(60) Li, C.; Wan, J.; Kalali, E. N.; Fan, H.; Wang, D.-Y. Synthesis and characterization of functional eugenol derivative based layered double hydroxide and its use as a nanoflame-retardant in epoxy resin. *J. Mater. Chem. A* **2015**, *3*, 3471−3479.
(61) Wang, X.; Zhou, S.; Xing, W.; Yu, B.; Feng, X.; Song, L.; Hu, Y. Self-assembly of Ni-Fe layered double hydroxide/graphene hybrids for reducing fire hazard in epoxy composites. *J. Mater. Chem. A* **2013**, *1*, 4383−4390.
(62) Morgan, A. B.; Gilman, J. W. An overview of flame retardancy of polymeric materials: application, technology, and future directions. *Fire Mater.* **2013**, *37*, 259−279.
(63) Sipinen, A. J.; Rutherford, D. R. A study of the oxidative degradation of polyolefins. *J. Environ. Polym. Degrad.* **1993**, *1*, 193−202.

DOI: 10.1021/acsomega.6b00485
ACS Omega 2017, 2, 20−31